Received: 14 March 2022 | Revised: 16 May 2022 | Accepted: 18 May 2022

DOI: 10.1002/gcc.23072

RESEARCH ARTICLE

WILEY

Inflammatory leiomyosarcoma/rhabdomyoblastic tumor: A report of two cases with novel genetic findings

Madina Sukhanova | Farres Obeidin | Lukas Streich | Borislav A. Alexiev

Department of Pathology, Northwestern University Feinberg School of Medicine, Northwestern Memorial Hospital, Chicago, Illinois, USA

Correspondence
Borislav A. Alexiev, Department of Pathology, Northwestern University Feinberg School of Medicine, Northwestern Memorial Hospital, 251 East Huron St, Feinberg 7-342A, Chicago, IL 60611, USA.
Email: borislav.alexiev@northwestern.edu

Abstract

Inflammatory leiomyosarcoma (ILMS) is a malignant neoplasm showing smooth muscle differentiation, a prominent inflammatory infiltrate, and near-haploidization. These tumors have significant pathologic and genetic overlap with the recently described "inflammatory rhabdomyoblastic tumor (IRT)," suggesting that ILMS and IRT may belong to one entity. Herein, we describe two cases of ILMS/IRT with attention to new cytogenetic and sequencing findings. The tumors were composed of sheets and fascicles of variably pleomorphic tumor cells showing spindled and epithelioid to rhabdoid morphology and a prominent histiocyte-rich inflammatory infiltrate typical of ILMS/IRT. In case 1, chromosomal microarray analysis showed a near-haploid pattern with loss of heterozygosity resulting from loss of one copy of all autosomes except for chromosomes 5, 20, 21, and 22. Case 2 showed areas with high-grade rhabdomyosarcomatous transformation. In this case, the low-grade tumor component revealed a hyper-diploid pattern with loss of heterozygosity for most of autosomes but with a normal diploid copy number state except for chromosomes 5, 20, and 22, which showed a relative gain. The high-grade tumor component showed a similar pattern of copy-neutral loss of heterozygosity with additional abnormalities, including mosaic segmental gains at 1p, 5p, 8q, 9p, 20q, and segmental loss at 8p. Next-generation sequencing identified sequence variants in *NF1*, *TP53*, *SMARCA4*, *KRAS*, and *MSH6*. *MSH6* variant was confirmed as germline, consistent with the diagnosis of hereditary nonpolyposis colorectal cancer (HNPCC) syndrome in one of our study patients and suggestive that ILMS/IRT might be part of the HNPCC cancer spectrum.

KEYWORDS
driver mutations, inflammatory leiomyosarcoma/rhabdomyoblastic tumor, inflammatory rhabdomyoblastic tumor

1 | INTRODUCTION

Inflammatory leiomyosarcoma (ILMS) is a malignant neoplasm showing smooth muscle differentiation, a prominent inflammatory infiltrate, and near-haploidization.[1–8] The tumor shows frequent co-expression of smooth and skeletal muscle markers supporting a primitive myogenic phenotype.[7] The presence of significant clinicopathologic and cytogenetic overlap of ILMS with the recently described "histiocyte-rich rhabdomyoblastic tumor (HRRMT)" have prompted discussion as to whether they fall under a single entity.[9–14] In a recent review,

Cloutier and colleagues proposed reclassification of ILMS and HRRMT as "inflammatory rhabdomyoblastic tumor" on the basis of chromosomal microarray studies showing concurrence of near-haploidization events in both tumors.[13] Currently, sequencing studies of ILMS/IRT for possible driver genes have been limited, with only recurrent *NF1* sequence variants reported.[8]

The purpose of this study is to provide comprehensive clinicopathologic and molecular characterization of two cases of ILMS/HRRMT diagnosed at our institution to identify additional molecular drivers that may have a significant prognostic value for ILMS/IRT patients, and to define their proper place in the classification of soft tissue neoplasms.

2 | MATERIALS AND METHODS

The present study was approved by the Institutional Review Board of Northwestern Memorial Hospital.

2.1 | Histology

Representative/extensive tissue sections from the surgical specimens were fixed in 10% buffered formalin and embedded in paraffin. For routine microscopy, 4-μm-thick sections were stained with hematoxylin–eosin.

2.1.1 | Immunohistochemistry

Immunohistochemical staining was performed using an automated immunostainer (Leica Bond-III, Leica Biosystems, Buffalo Grove, IL) and Bond Refine PolymerTM biotin-free DAB detection kit. Formalin-fixed, paraffin-embedded tissue sections were stained with desmin (mouse monoclonal, DE-R-11, predilute ready-to-use, Ventana, Oro Valley, AZ), h-caldesmon (mouse monoclonal, h-CALD, 1:400 dilution, Thermo Fisher, Waltham, MA), smooth muscle actin (mouse monoclonal, 1A4, predilute ready-to-use, Rocklin, CA), MyoD1 (rabbit monoclonal, Ep212, predilute ready-to-use, Rocklin, CA), myogenin (mouse monoclonal, FSD, predilute ready-to-use, Ventana, Oro Valley, AZ), MLH1 (mouse monoclonal, ES05, Leica Biosystems, Buffalo Grove, IL), MSH2 (mouse monoclonal, 79H11, Leica Biosystems, Buffalo Grove, IL), MSH6 (rabbit monoclonal, EP49, Leica Biosystems, Buffalo Grove, IL), PMS2 (mouse monoclonal, EP51, Leica Biosystems, Buffalo Grove, IL). A positive nuclear, cytoplasmic and/or membranous expression was identified in 10% or more of neoplastic cells qualified as "positive (+)."

2.1.2 | DNA isolation, chromosomal microarray analysis, and next generation sequencing

Genomic DNA was extracted from formalin-fixed, paraffin-embedded (FFPE) tissue using a Qiagen AllPrep DNA/RNA FFPE Kit (Qiagen, Valencia, CA), following the manufacturer's protocol. Prior to DNA extraction, tissue was deparaffinized using Hemo D, 100% ethanol and digested at 37°C in Qiagen Tissue lysis buffer and proteinase K. DNA was quantified by Qubit 3.0 (Thermo Scientific, Waltham, MA).

Chromosomal microarray analysis (CMA) was performed using the Affymetrix OncoScan^{R} CNV array (Thermo Fisher Scientific, Santa Clara, CA), following the manufacturer's protocol. The data were analyzed with the Affymetrix Chromosome Analysis Suite (ChAS) software.

The DNA portion of the Comprehensive Cancer Next Generation Sequencing (NGS) was performed following the manufacturer's instruction, using DNA primers (ThermoFIsher Scientific, Waltham, MA).

This panel is an amplification based NGS test, designed to detect mutations within targeted areas, full exons, copy numbers, and fusions of current clinical relevance in 161 genes (Table S1). This assay utilizes the Ion Torrent targeted amplification system using the Ion S5 xl next generation sequencer.

3 | RESULTS

3.1 | Case 1

3.1.1 | Clinical findings

The first patient is a 64-year-old male with a past medical history of diffuse large B cell lymphoma status post autologous stem cell transplant who presented with a 2.1 cm mass within the right psoas muscle.

3.1.2 | Histology and immunohistochemistry

Histological analysis of resection specimen showed a neoplasm composed of spindle cells with blunt-ended nuclei, small nucleoli, and eosinophilic cytoplasm arranged in fascicles. Scattered rhabdoid cells with brightly eosinophilic cytoplasm were also noted. The neoplastic cells were admixed with a dense mixed inflammatory infiltrate composed of histiocytes, lymphocytes, plasma cells, and eosinophils. Calcospherites were scattered throughout the lesion. Rare mitotic figures (3/10 high power fields) could be seen, and no tumor necrosis was present. Immunohistochemical stains revealed expression of desmin, h-caldesmon, and MyoD1, but not myogenin (Figure 1A–D).

3.1.3 | Genomic data

CMA for case 1 showed a near-haploid pattern with loss of heterozygosity (LOH) resulting from loss of one copy of all autosomes except for chromosomes 5, 20, 21, and 22, which retained normal diploid state (Figure 2).

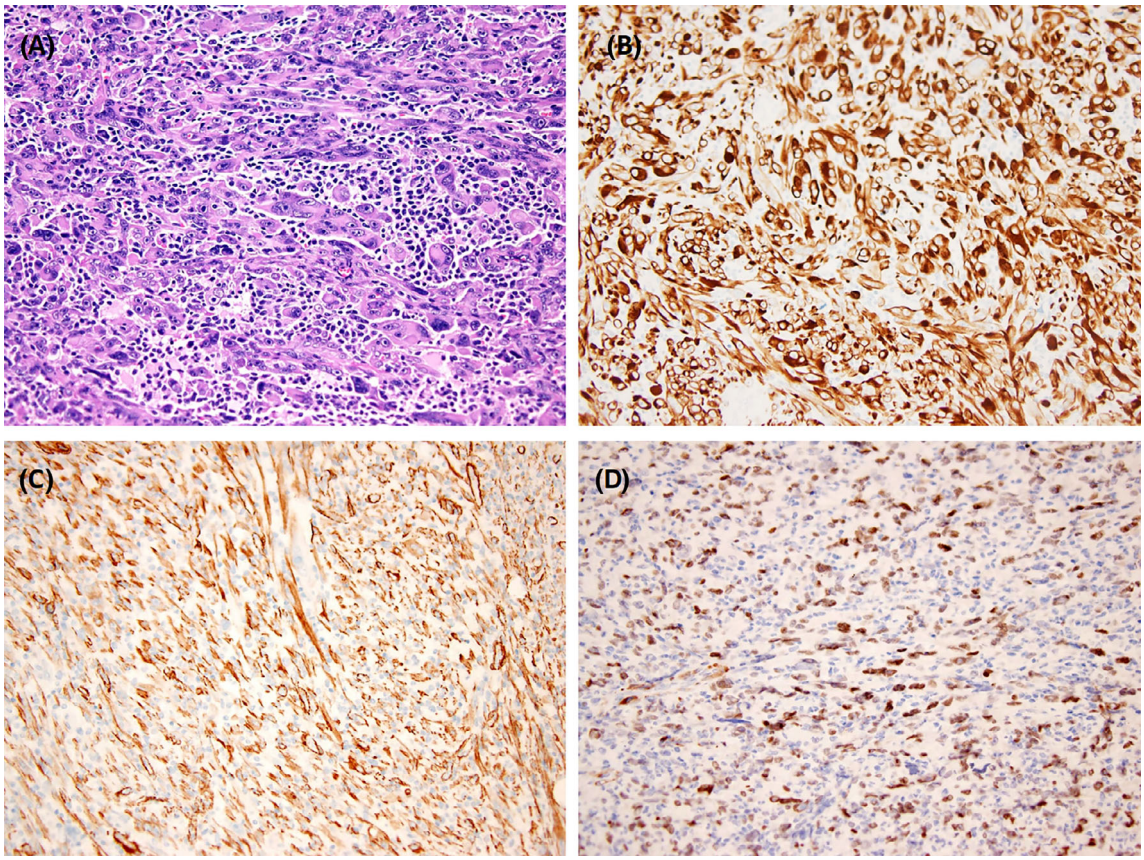

FIGURE 1 Case 1. (A) Tumor is composed of tumor cells showing spindled and epithelioid to rhabdoid morphology, eosinophilic cytoplasm, and prominent nucleoli, arranged in fascicles. A prominent inflammatory cell infiltrate is present. Hematoxylin and eosin stain, ×200. (B) Desmin expression in tumor cells. Desmin stain, ×200. (C) H-caldesmon expression in tumor cells. H-caldesmon stain, ×200. (D) MyoD1 expression in tumor cells. MyoD1 stain, ×200

NGS testing identified 6 non-synonymous sequence variants in case 1, 3 of which were classified as pathogenic and listed in the Table 1. Comparison of allelic frequencies revealed that pathogenic clinically significant variants in *NF1* (located at chromosome band 17q11.2, 34%) and *TP53* (17p13.3, 27%) likely belong to a predominant clone (with an average allele frequency between these two variants at ~30.5%). An additional mutation detected was a frameshift variant in *SMARCA4* (19p13.2), noted at allelic frequency of 6%, suggestive of a secondary sub-clone. Missense variants in *SLX4* (A251V, 16p13.3), *FANCA* (D953E, 16q24.3), and *ESR1* (R269C, 6q25.1-q25.2) identified in this case were evaluated as variants of unknown clinical significance based on currently available information including population databases (gnomAD, ExAc, and dbSNP), databases of somatic variants associated with cancer (COSMIC), ClinVar, in silico prediction tools, and published functional studies and not included in Table 1.

3.1.4 | Diagnosis and treatment

The morphological features, immunohistochemical profile, and CMA results supported a diagnosis of ILMS/IRT. The tumor was completely resected with negative surgical margins, and follow-up PET-CT showed no evidence of metastatic disease at 5 months after surgery.

3.2 | Case 2

3.2.1 | Clinical findings

The patient is a 23-year-old female presented with multiple subcentimeter breast and lung nodules and an 11.5 cm mass in the left vastus lateralis muscle.

3.2.2 | Histology and immunohistochemistry

Histological analysis of resection specimen showed a neoplasm composed of spindle cells with blunt-ended nuclei, small nucleoli, and eosinophilic cytoplasm arranged in fascicles. Scattered rhabdoid cells with eosinophilic cytoplasm and multinucleated cells with large vesicular nuclei and prominent nucleoli were also noted. The neoplastic cells were admixed with a dense mixed inflammatory infiltrate composed of histiocytes, lymphocytes, plasma cells, and eosinophils.

FIGURE 2 Case 1. Chromosomal microarray whole-genome profile of the tumor

TABLE 1 Mutations detected by NGS

	Case 1	Case 2	
		Low-grade component	High-grade component
The list of detected variants	*TP53* p.V143A (27%) NM_000546.5	*TP53* p.R273H (45%) NM_000546.5	*TP53* p.R282W (17%) NM_000546.5
	NF1 p.E1210fs (34%) NM_001042492.2	*NF1* p.R192* (38%) NM_001042492.2	*NF1* p.R192* (17%) NM_001042492.2
	SMARCA4 p.E952fs (6%) NM_001128849.1	*MSH6* p.? (splice site) (67%) NM_000179.2	*MSH6* p.? (splice site) (55%) NM_000179.2
		KRAS p.V14I (40%)	

Calcospherites were scattered throughout the lesion. This spindle cell component was mixed with solid areas showing more prominent pleomorphism, numerous mitotic figures (>30/10 high power fields, including atypical mitoses), and marked tumor necrosis. Immunohistochemistry revealed expression of desmin and MyoD1 but not h-caldesmon and myogenin (Figure 3A–D). The tumor showed loss of nuclear MSH6 expression and retained MLH1, MSH2, and PMS2.

3.2.3 | Genomic data

CMA was performed separately on both tumor components (Figure 4). The low-grade tumor component revealed a hyper-diploid pattern with LOH pattern for most autosomes but with a normal diploid copy number state, a phenomenon known as copy-neutral *LOH* (CN-LOH). This finding was in all autosomes except for chromosomes 5, 20, and 22 which showed a relative gain. This plot pattern is suggestive of a doubling of a near-haploid clone. Independent analysis of the morphologically high-grade tumor component revealed a similar global CN-LOH plot with additional segmental copy number abnormalities, including relative mosaic segmental gains at 1p, 5p, 8q, 9p, 20q, and relative segmental loss at 8p (Figure 5). Comparative analysis of global CN-LOH patterns in low- and high-grade components is suggestive that the tumors are likely clonally related with Allele Difference profile of high-grade component showing more complex pattern of aberrations, including segmental losses at 5q and 20p, likely as a secondary event occurring during tumor progression.

NGS testing of case 2 identified four sequence changes (Table 1). Similar to case 1, this case revealed a predominant clone with loss-of-function variants in *NF1* (17q11.2) and *TP53* (17p13.3) in ~41.5%

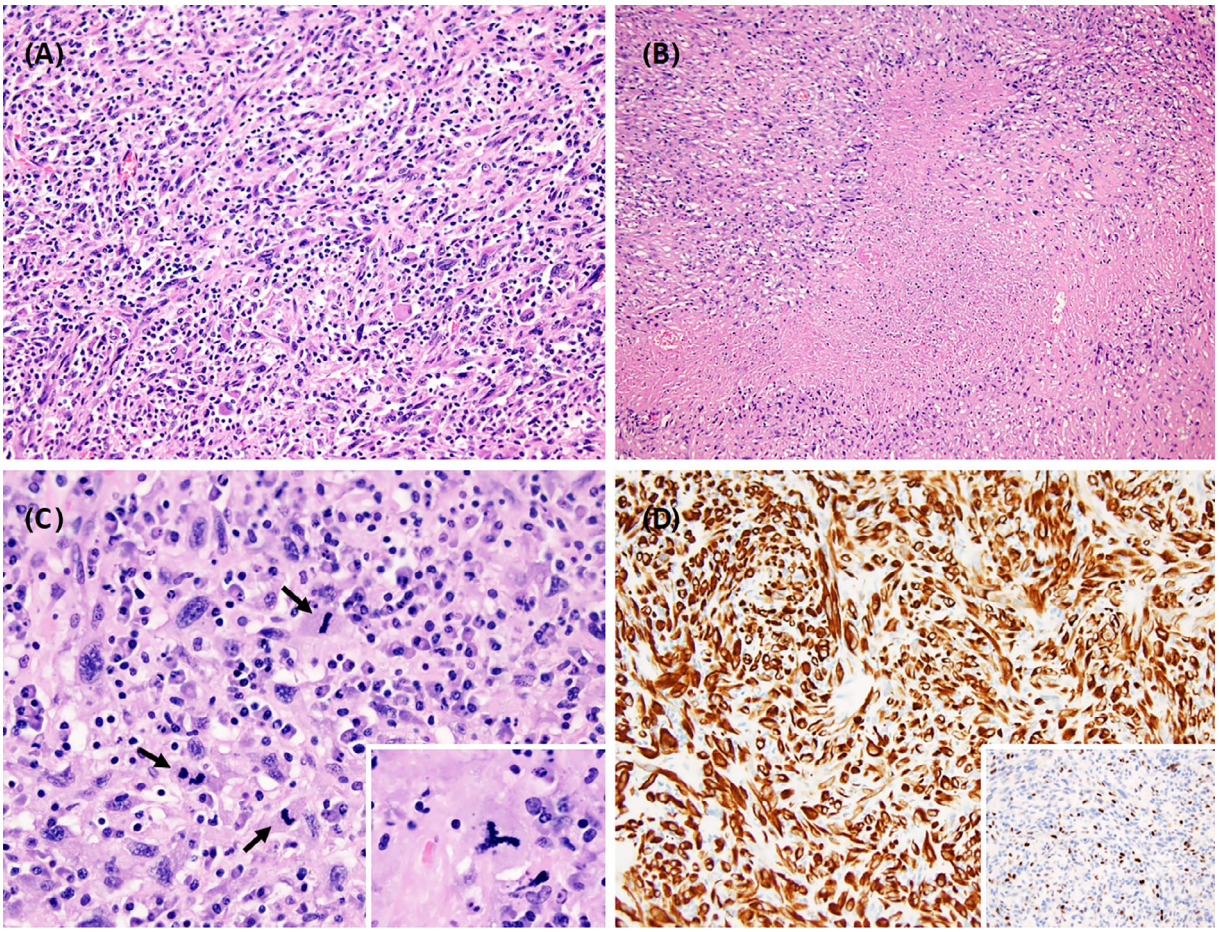

FIGURE 3 Case 2. (A) Tumor is composed of tumor cells showing spindled and epithelioid to rhabdoid morphology, eosinophilic cytoplasm, and prominent nucleoli, arranged in fascicles. A prominent inflammatory cell infiltrate is present. Hematoxylin and eosin stain, ×200. (B) Area with high-grade rhabdomyosarcomatous transformation. Note extensive necrosis. Hematoxylin and eosin, ×200. (C) Area with high- grade rhabdomyosarcomatous transformation. Note increased mitotic activity (arrow) and atypical mitosis (inset) Hematoxylin and eosin stain, ×200 and ×400 (inset). (D) Desmin and MyoD1 (inset) expression in tumor cells. Desmin and MyoD1 stains, ×200.

average proportion of sequencing reads. Comparative analysis of low-grade component versus high-grade tumor component revealed that both components shared the same truncating variant in *NF1* and the same splice-site variant in *MSH6* (2p16.3). Notably, splice site variant in the *MSH6* gene was noted in a high proportion of sequencing reads (67%). This finding and an early-onset of cancer in this patient prompted us to perform NGS of normal muscle biopsy, which confirmed germline origin of this splice-site variant in *MSH6* with expected allele frequency in normal tissue at 50%. This variant c.3172+1G>T in *MSH6* disrupts a donor splice site in intron 4 is expected to affect mRNA processing and lead to aberrant splicing with resulting exon-skipping events and protein truncation. This particular change was reported in individuals affected with Lynch syndrome and is reported in five entries in ClinVar (Variation ID: 89344) as a variant of clinical significance.[15] Follow-up immunohistochemical testing showed loss of the MSH6 protein in tumor and non-tumor tissue, confirming the functional deficiency in this patient's tumor.

The low-grade and high-grade tumor components demonstrated different pathogenic *TP53* variants (R273H and R282W, respectively), and only the low-grade component showed a *KRAS* variant (V14I). An additional variant (Q894H) in *MSH6*, noted in high-grade component only, was classified as a variant of unknown clinical significance based on the same criteria described above and not included in Table 1.

It should also be noted that due to loss of chromosomes 17 and 19 in case 1 and CN-LOH affecting both chromosomes in case 2, true frequencies of detected variants of clinical significance in *TP53* and *NF1* are halved.

3.2.4 | Diagnosis and treatment

The morphological features, immunohistochemical profile, and CMA results supported a diagnosis of ILMS/IRT with high-grade rhabdomyosarcomatous transformation. Following complete resection of the tumor with negative surgical margins, the patient was treated for a high-grade metastatic sarcoma with doxorubicin, ifosfamide, and mesna chemotherapy. The patient is currently alive with stable disease on CT 6 months following treatment.

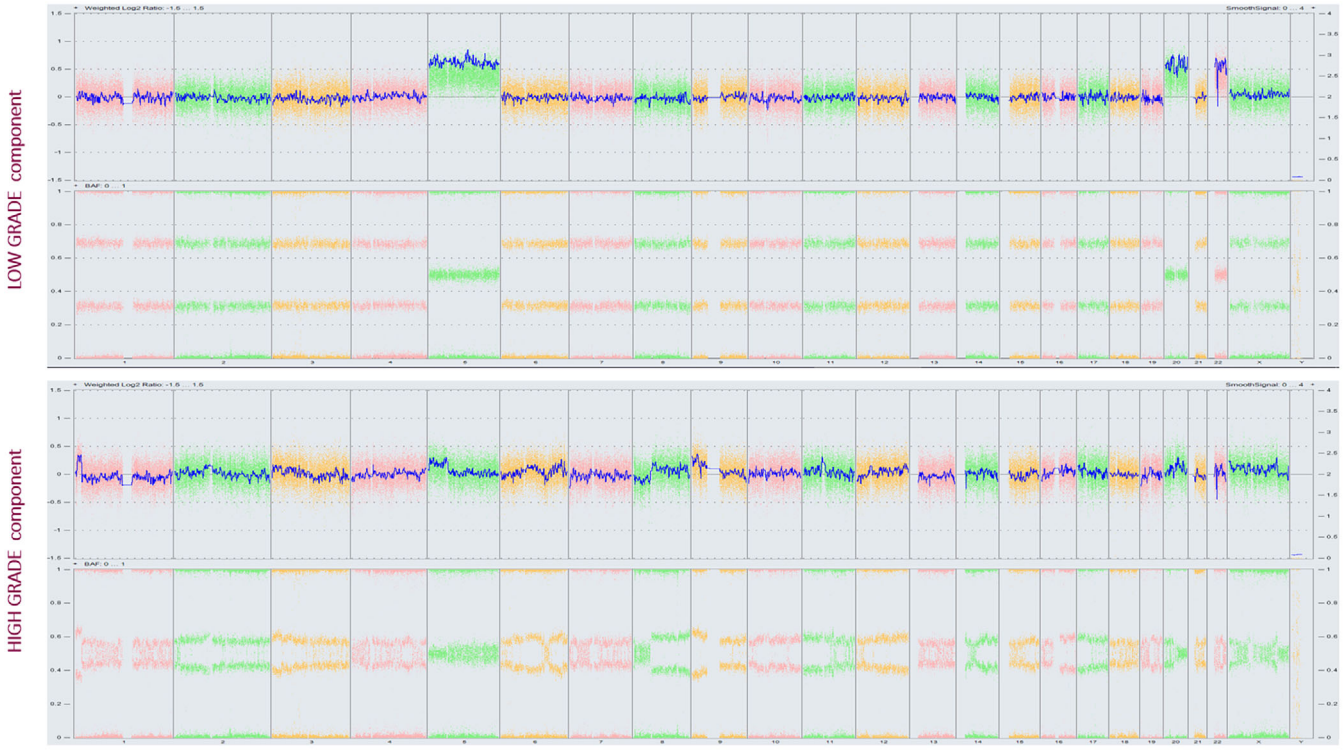

FIGURE 4 Case 2. Chromosomal microarray whole-genome view plot. Profile of low-grade and high-grade tumor components

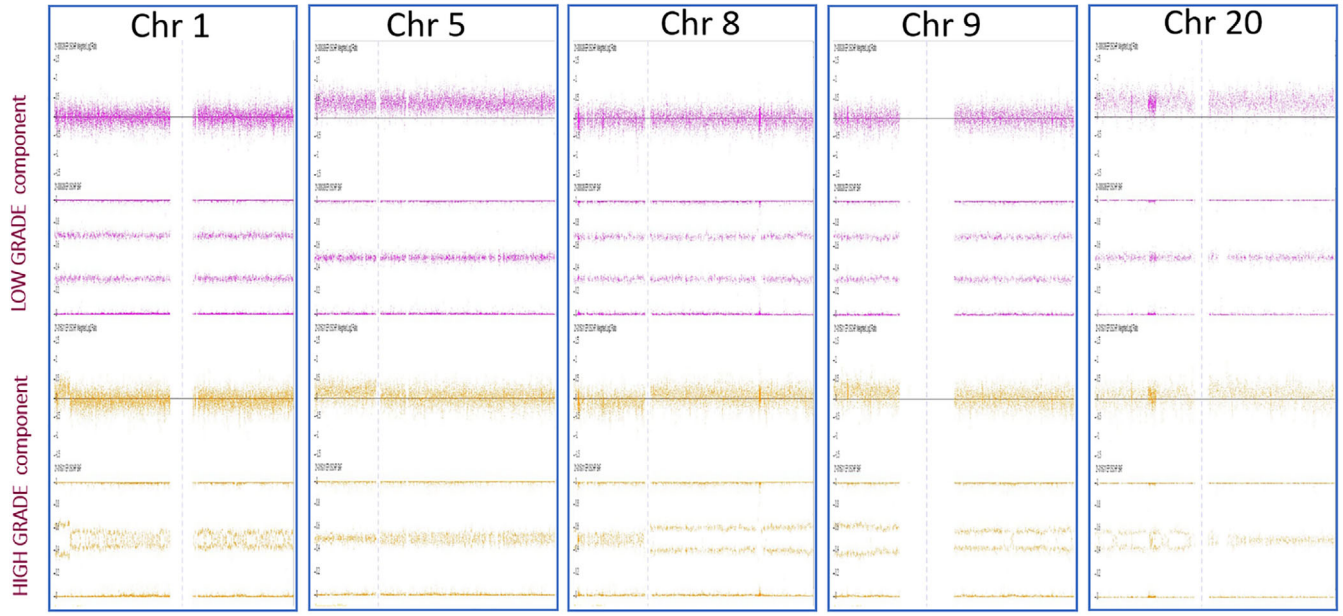

FIGURE 5 Case 2. Detailed comparison of chromosomal microarray whole-genome view plots for chromosomes 1, 5, 8, 9, and 20. Top panel: low-grade tumor component; bottom panel: high-grade tumor component

4 | DISCUSSION

Both tumors demonstrated characteristic features of ILMS/IRT: They were composed of variably pleomorphic tumor cells showing spindled and epithelioid to rhabdoid morphology, eosinophilic cytoplasm, and prominent nucleoli arranged in fascicles. A prominent histiocyte-rich inflammatory cell infiltrate was evident, often obscuring the neoplastic cells. One of the tumors showed areas with geographic necrosis and markedly increased mitotic activity, including atypical mitoses, consistent with high-grade rhabdomyosarcomatous transformation.

Immunohistochemical stains showed that the tumors cells stained positively for desmin and MyoD1 and were negative for myogenin; additionally, one of the tumors was positive for h-caldesmon. CD163 and CD168 were expressed in stromal histiocytes. The observed morphologic and immunophenotypic features of both tumors show overlap of smooth and skeletal muscle phenotypes, in agreement with prior literature on ILMS/IRT.[7]

The characteristic genetic finding previously described in ILMS/IRT is a near-haploid loss of heterozygosity, which was seen in case 1 of this study.[1,3,4,6] A recent report by Geiersbach et al. echoes the findings in our second case, defined by the presence of a high-grade component with a hyperdiploid plot with widespread LOH suggesting whole genome duplication following the initial haploidization.[14] Apart from the cytogenetic findings, data is currently very limited on gene sequence aberrations. The two cases we present provide insight into the pathogenesis of ILMS/IRT and identify possible diagnostic and prognostic markers for future studies and targeted therapies.

In agreement with previous observations, mutations in the tumor suppressor *NF1* were detected in both cases with ILMS/IRT.[6,8,9] This *gene* produces neurofibromin, a protein with *oncosuppressive* activity that helps regulate cell growth and is a negative feedback regulator of the RAS–MAPK signaling pathway. Mutations of the *NF1* tumor suppressor gene predispose individuals to a variety of benign and malignant tumors, including rhabdomyosarcoma.[15]

Our study is the first one to demonstrate *TP53* mutations in ILMS/IRT. Both genes, *TP53* and *NF1*, are located on chromosome 17. Loss of one chromosome 17 and pathogenic mutations of both genes on the remaining homolog were noted in one case and mutations of both genes with concurrent CN-LOH pattern affecting entire chromosome 17 was detected in the other. As a result, both cases demonstrated a bi-allelic loss of both tumor suppressors. *TP53* plays a critical role in protecting the cell from the transformative effects of DNA damage by inducing cell-cycle arrest and apoptosis. Loss of *TP53* function is associated with genomic instability and the development of aneuploidy in cancer.[15–21] An interesting association is loss of *TP53* together with hypodiploidy. In this context, DNA hypodiploidy is a unique and rare finding associated with loss chromosome 17/*TP53* mutations and aggressive behavior/poor outcome in solid tumors and hematologic malignancies like hypodiploid acute lymphoblastic leukemia (ALL). It has been surmised in ALL with hypodiploidy that the loss of multiple chromosomes likely occurs secondary to mitotic nondisjunction in the absence of *TP53* tumor suppressor function. Whole-genome doubling is also reported in cases of hypodiploid ALL, masking the original hypodiploid population of cells.[20,21] These findings suggest that alterations of *TP53* function may promote the characteristic hypodiploidy in ILMS/IRT. We hypothesize that in ILMS/IRT, cells first acquire *NF1* mutation and then, following loss of *TP53*, undergo further clonal evolution through erroneous nondisjunction resulting in near-haploidization. Whole genome reduplication of the original near-haploid clone (pseudo-hyperdiploidy) which was seen in our second case may be a stepwise event associated with tumor progression. In addition to the loss of *TP53* tumor suppressor function, alternative mechanisms may contribute to the functional impairment of the p53 pathway.

An additional mutation detected in our study was a frameshift variant in *SMARCA4* (19p13.2), which encodes an ATPase subunit of BAF chromatin-remodeling complexes. Inactivation of *SMARCA4* has been reported in a wide variety of cancers and is often characterized by a high-grade undifferentiated or rhabdoid histomorphology as seen in small cell carcinoma of the ovary hypercalcemic type and *SMARCA4*-deficient thoracic and uterine sarcomas.[22–25] The clinical hallmarks of these tumors include a limited response to chemotherapy and rapid local progression.

A splice-site mutation of potential clinical significance in *MSH6* was noted in both low-grade and high-grade tumor components and has not been reported in ILMS/IRT previously. The *MSH6* gene is located at the chromosomal band 2p16.3. Detection of this splice-site variant in *MSH6* in low-grade tumor component in a high proportion of sequencing reads greater than 50% (67%) and CN-LOH event affecting chromosome 2 is consistent with a homozygous state of this variant in tumor cells, adding to tumor pathogenesis. Most notably, we confirmed germline origin of this *MSH6* splice-site mutation adding this rare tumor type to the cancer spectrum of hereditary non-polyposis colorectal cancer (HNPCC) syndrome, known as Lynch syndrome. Germline mutations in any of the four-mismatch repair (MMR) genes, *MLH1*, *MSH2*, *MSH6*, and *PMS2*, are the underlying cause of hereditary nonpolyposis colorectal cancer (HNPCC) syndrome, known as Lynch syndrome.[26–33] Subjects carrying a mutation in one of the MMR genes have a high risk of developing colorectal or endometrial cancer, as well as several other cancers.[28] Female *MSH6* mutation carriers have a higher risk for developing endometrial carcinoma.[27] These observations provide a basis for which mismatch repair protein screening in ILMS/IRT may be considered. The clinical pathogenicity of this splice-site variant was confirmed by careful review of available information in ClinVar, and functionality was demonstrated by loss of MSH6 staining on immunohistochemistry. It is pivotal for the clinical management of patients with *MSH6* mutations to have a clear genetic diagnosis since they may benefit from screening, preventive, and personal therapeutic measures.[26–31] Microsatellite instability in colorectal cancer is often associated with local strong lymphocyte infiltration and low frequency of distant metastases, and a dense lymphocytic infiltrate was also noted in the *MSH6*-mutated ILMS/IRT case in our study.[26,33]

Mutations in the *KRAS* oncogene are present in up to 25% of all human tumors but are rare in soft tissue sarcomas.[34–37] We demonstrate here the presence of a *KRAS* p.V14I pathogenic variant in a case of ILMS/IRT with high-grade transformation. Lung cancers with *KRAS* point mutations have worse prognosis and a tendency to be smaller and less differentiated than those without mutations.[36] Moreover, lung and colon carcinomas with *KRAS* mutation may be resistant to epidermal growth factor receptor tyrosine kinase inhibitors.[35] Further study is needed to determine the full therapeutic implications of mutations in this gene in ILMS/IRT.

The p.D953E variant in *FANCA* is of particular interest. Variants in *FANCA* have not been reported in ILMS/IRT. The gene plays an essential *role in maintaining genome stability and* modulating responses to endogenous aldehydes, oxidative stress, and inflammation. Various mutations in *FANCA* are observed in Fanconi anemia and malignant

neoplasms such as endometrial and gastrointestinal cancer.[38–43] Two-thirds of Fanconi anemia patients harbor pathogenic variants in *FANCA*, which makes it the most frequently mutated Fanconi anemia gene.[42] Although the identified variant in *FANCA*, D953E, does not lie within any reported functional domains of the protein, it has been shown that this particular sequence change does not fully complement survival of *FANCA*-deficient cells after mitomycin C treatment; thus, further functional characterization is needed.[43] If proven pathogenic, the identified *variant* might have an impact on host's *immune/inflammatory response to tumor growth. Further* carefully designed *studies* are necessary to demonstrate the relationship between *FANCA* mutations and the prominent, diffuse inflammatory response to tumor cells in ILMS/IRT.

5 | CONCLUSION

The results of our small study set describe both oncogenic mutations (*KRAS*, *TP53*) as well as mutations in genes essential to maintaining genome stability and modulating host immune responses to tumor growth (*FANCA*, *MSH6*) in ILMS/IRT. These findings have profound implications for our understanding of the genetic pathogenesis and characteristic karyotypic changes of these neoplasms. These data support the notion that patients with ILMS/IRT may have a variable clinical course. Some behave in an indolent manner while others show progression to aggressive sarcomas with additional mutations affecting metastatic potential and sensitivity to conventional therapies.[5,14] *MSH6* variant was confirmed as germline, consistent with the diagnosis of HNPCC syndrome in one of our study patients and suggestive that ILMS/IRT might be part of the HNPCC cancer spectrum. Further study of ILMS/IRT with additional cases and longer follow-up is warranted to better understand the biologic behavior of these tumors.

DATA AVAILABILITY STATEMENT

Data available on request from the authors.

ORCID

Madina Sukhanova https://orcid.org/0000-0002-1843-7038
Farres Obeidin https://orcid.org/0000-0001-8461-9238
Borislav A. Alexiev https://orcid.org/0000-0002-0262-2263

REFERENCES

1. Fletcher CDM, Mertens F. Inflammatory leiomyosarcoma. In: The WHO Classification of Tumours Editorial Board, ed. *WHO classification of tumours: Soft tissue and bone tumours*. 5th ed. International Agency for Research on Cancer; 2019:193-194.
2. Merchant W, Calonje E, Fletcher CD. Inflammatory leiomyosarcoma: a morphological subgroup within the heterogeneous family of so-called inflammatory malignant fibrous histiocytoma. *Histopathology*. 1995;27(6):525-532.
3. Nord KH, Paulsson K, Veerla S, et al. Retained heterodisomy is associated with high gene expression in hyperhaploid inflammatory leiomyosarcoma. *Neoplasia*. 2012;14(9):807-812.
4. Dal Cin P, Sciot R, Fletcher CD, et al. Inflammatory leiomyosarcoma may be characterized by specific near-haploid chromosome changes. *J Pathol*. 1998;185(1):112-115.
5. Chang A, Schuetze SM, Conrad EU 3rd, Swisshelm KL, Norwood TH, Rubin BP. So-called "inflammatory leiomyosarcoma": a series of 3 cases providing additional insights into a rare entity. *Int J Surg Pathol*. 2005;13(2):185-195.
6. Lee JC, Li WS, Kao YC, Chung YC, Huang HY. Toward a unifying entity that encompasses most, but perhaps not all, inflammatory leiomyosarcomas and histiocyte-rich rhabdomyoblastic tumors. *Mod Pathol*. 2021;34(7):1434-1438.
7. Michal M, Rubin BP, Kazakov DV, et al. Inflammatory leiomyosarcoma shows frequent co-expression of smooth and skeletal muscle markers supporting a primitive myogenic phenotype: a report of 9 cases with a proposal for reclassification as low-grade inflammatory myogenic tumor. *Virchows Arch*. 2020;477(2):219-230.
8. Arbajian E, Köster J, Vult von Steyern F, Mertens F. Inflammatory leiomyosarcoma is a distinct tumor characterized by near-haploidization, few somatic mutations, and a primitive myogenic gene expression signature. *Mod Pathol*. 2018;31(1):93-100.
9. Xia Y, Li Y, Gong P, Jiang H, Zhang X. Clinicopathological analysis and genomic profiling of a rare histiocyte-rich rhabdomyoblastic tumor: a case report. *Medicine*. 2021;100(24):e26105.
10. Bourgeau M, Martinez AP. Histiocyte-rich rhabdomyoblastic tumor: a report of two cases and a review of the differential diagnoses. *Virchows Arch*. 2021;478(2):367-373.
11. Folpe AL. Response to Lee et al: toward a unifying entity that encompasses most, but perhaps not all, inflammatory leiomyosarcomas and histiocyte-rich rhabdomyoblastic tumors. *Mod Pathol*. 2021;34(7):1439.
12. Martinez AP, Fritchie KJ, Weiss SW, et al. Histiocyte-rich rhabdomyoblastic tumor: rhabdomyosarcoma, rhabdomyoma, or rhabdomyoblastic tumor of uncertain malignant potential? A histologically distinctive rhabdomyoblastic tumor in search of a place in the classification of skeletal muscle neoplasms. *Mod Pathol*. 2019;32(3):446-457.
13. Cloutier JM, Charville GW, Mertens F, et al. Inflammatory Leiomyosarcoma" and "Histiocyte-rich Rhabdomyoblastic Tumor": a clinicopathological, immunohistochemical and genetic study of 13 cases, with a proposal for reclassification as "Inflammatory Rhabdomyoblastic Tumor. *Mod Pathol*. 2021;34(4):758-769.
14. Geiersbach K, Kleven DT, Blankenship HT, Fritchie K, Folpe AL. Inflammatory rhabdomyoblastic tumor with progression to high-grade rhabdomyosarcoma. *Mod Pathol*. 2021;34(5):1035-1036.
15. Pillozzi S, Bernini A, Palchetti I, et al. Soft tissue sarcoma: an insight on biomarkers at molecular, metabolic and cellular level. *Cancer*. 2021;13(12):3044.
16. Thompson SL, Compton DA. Proliferation of aneuploid human cells is limited by a p53-dependent mechanism. *J Cell Biol*. 2010;188(3):369-381.
17. Zhou X, Hao Q, Lu H. Mutant p53 in cancer therapy-the barrier or the path. *J Mol Cell Biol*. 2019;11(4):293-305.
18. Thoenen E, Curl A, Iwakuma T. TP53 in bone and soft tissue sarcomas. *Pharmacol Ther*. 2019;202:149-164.
19. Pérot G, Chibon F, Montero A, et al. Constant p53 pathway inactivation in a large series of soft tissue sarcomas with complex genetics. *Am J Pathol*. 2010;177(4):2080-2090.
20. El-Naggar AK, Dinh M, Tucker SL, Swanson D, Steck K, Vielh P. Numerical chromosomal changes in DNA hypodiploid solid tumors: restricted loss and gain of certain chromosomes. *Cytometry*. 1999;37(2):107-112.
21. Comeaux EQ, Mullighan CG. *TP53* mutations in hypodiploid acute lymphoblastic leukemia. *CSH Perspect Med*. 2017;7(3):a026286.
22. Le Loarer F, Watson S, Pierron G, et al. SMARCA4 inactivation defines a group of undifferentiated thoracic malignancies transcriptionally related to BAF-deficient sarcomas. *Nat Genet*. 2015;47(10):1200-1205.
23. Sauter JL, Graham RP, Larsen BT, Jenkins SM, Roden AC, Boland JM. SMARCA4-deficient thoracic sarcoma: a distinctive

clinicopathological entity with undifferentiated rhabdoid morphology and aggressive behavior. *Mod Pathol*. 2017;30(10):1422-1432.
24. Mardinian K, Adashek JJ, Botta GP, Kato S, Kurzrock R. *SMARCA4*: implications of an altered chromatin-remodeling gene for cancer development and therapy. *Mol Cancer Ther*. 2021;20(12):2341-2351.
25. Roden AC. Thoracic SMARCA4-deficient undifferentiated tumor—a case of an aggressive neoplasm-case report. *Mediastinum*. 2021;5:39.
26. Buckowitz A, Knaebel HP, Benner A, et al. Microsatellite instability in colorectal cancer is associated with local lymphocyte infiltration and low frequency of distant metastases. *Br J Cancer*. 2005;92(9):1746-1753.
27. Ramsoekh D, Wagner A, van Leerdam ME, et al. Cancer risk in MLH1, MSH2 and MSH6 mutation carriers; different risk profiles may influence clinical management. *Hered Cancer Clin Pract*. 2009;7(1):17.
28. Frederiksen JH, Jensen SB, Tümer Z, Hansen TVO. Classification of MSH6 variants of uncertain significance using functional assays. *Int J Mol Sci*. 2021;22(16):8627.
29. Pagenstecher C, Wehner M, Friedl W, et al. Aberrant splicing in MLH1 and MSH2 due to exonic and intronic variants. *Hum Genet*. 2006;119(1–2):9-22.
30. Segura SE, Pedra Nobre S, Hussein YR, et al. DNA mismatch repair-deficient endometrial carcinosarcomas portend distinct clinical, morphologic, and molecular features compared with traditional carcinosarcomas. *Am J Surg Pathol*. 2020;44(11):1573-1579.
31. Hoang LN, Ali RH, Lau S, Gilks CB, Lee CH. Immunohistochemical survey of mismatch repair protein expression in uterine sarcomas and carcinosarcomas. *Int J Gynecol Pathol*. 2014;33(5):483-491.
32. Chang EY, Dorsey PB, Frankhouse J, et al. Combination of microsatellite instability and lymphocytic infiltrate as a prognostic indicator in colon cancer. *Arch Surg*. 2009;144(6):511-515.
33. Talseth-Palmer BA, McPhillips M, Groombridge C, Spigelman A, Scott RJ. MSH6 and PMS2 mutation positive Australian Lynch syndrome families: novel mutations, cancer risk and age of diagnosis of colorectal cancer. *Hered Cancer Clin Pract*. 2010;8(1):5.
34. Li B, Li L, Li X, et al. Undifferentiated pleomorphic sarcoma with co-existence of KRAS/PIK3CA mutations. *Int J Clin Exp Pathol*. 2015;8(7):8563-8567.
35. Beganoyic S. Clinical significance of the KRAS mutation. *Bosn J Basic Med Sci*. 2009;9(Suppl 1):S17-S20.
36. Salgia R, Pharaon R, Mambetsariev I, Nam A, Sattler M. The improbable targeted therapy: KRAS as an emerging target in non-small cell lung cancer (NSCLC). *Cell Rep Med*. 2021;2(1):100186.
37. Hill MA, Gong C, Casey TJ, et al. Detection of K-ras mutations in resected primary leiomyosarcoma. *Cancer Epidemiol Biomarkers Prev*. 1997;6(12):1095-1100.
38. Kim Y, Lach FP, Desetty R, Hanenberg H, Auerbach AD, Smogorzewska A. Mutations of the SLX4 gene in Fanconi anemia. *Nat Genet*. 2011;43(2):142-146.
39. Young SJ, West SC. Coordinated roles of SLX4 and MutSβ in DNA repair and the maintenance of genome stability. *Crit Rev Biochem Mol Biol*. 2021;56(2):157-177.
40. Brégnard C, Guerra J, Déjardin S, Passalacqua F, Benkirane M, Laguette N. Upregulated LINE-1 activity in the Fanconi anemia cancer susceptibility syndrome leads to spontaneous pro-inflammatory cytokine production. *EBioMedicine*. 2016;8:184-194.
41. Del Valle J, Rofes P, Moreno-Cabrera JM, et al. Exploring the role of mutations in Fanconi anemia genes in hereditary cancer patients. *Cancer*. 2020;12(4):829.
42. Bagby G. Recent advances in understanding hematopoiesis in Fanconi anemia. *F1000Res*. 2018;7:105.
43. Kimble DC, Lach FP, Gregg SQ, et al. A comprehensive approach to identification of pathogenic FANCA variants in Fanconi anemia patients and their families. *Hum Mutat*. 2018;39(2):237-254.

SUPPORTING INFORMATION

Additional supporting information may be found in the online version of the article at the publisher's website.

How to cite this article: Sukhanova M, Obeidin F, Streich L, Alexiev BA. Inflammatory leiomyosarcoma/rhabdomyoblastic tumor: A report of two cases with novel genetic findings. *Genes Chromosomes Cancer*. 2022;61(11):653-661. doi:10.1002/gcc.23072